7) Mandersloot, W. G. B.: *Bull. Chem. Soc. Japan*, **37**, 1442 (1964)
8) Mizutani, Y., Watanabe,T.: private communication in 1968 (Odawara Salt Pilot Plant, Japan Monopoly Corporation)
9) Neihof, R., Sollner, K.: *J. Phys. Chem.*, **61**, 159 (1957)
10) Oda, Y.: *Reps. Res. Lab., Asahi Glass Co., Ltd. (Asahi Garasu Kenkyu Hōkoku)*, **16**, 37 (1966)
11) Peers, A. M.: *J. Appl. Chem.*, **8**, 57 (1958)
12) Scatchard, G., Hellferich, F.: *Disc. Faraday Soc.*, **21**, 70 (1956)
13) Seko, M.: Dechema Monographien, Band **47**, 575 (1962)
14) Tsunoda, Y., Kato, M.: *Desalination*, **3**, 66 (1967)

15) Weiner, S. A.: *Ind. Eng. Chem., Process Design and Develop.*, **4**, 349 (1965)
16) Wyllie, M. R. J.: *J. Phys. Chem.*, **58**, 67 (1954)
17) Wyllie, M. R. J., Kannan, S. L.: *J. Phys. Chem.*, **58**, 73 (1954)
18) Yamabe, T., Seno, M.: Ion Kōkan Jushimaku (Ion Exchange Resin Membrane), pp. 138-165 (1964) Gihōdō Book, Tokyo
19) Yawataya, T., Hani, H., Oda, Y., Nishihara, A.: Dechema Monographien, Band **47**, 501 (1962)
20) Wilson, J. R., ed.: Demineralization by Electrodialysis, Chap. 2, (1960), Butterworths, London

GAS ABSORPTION WITH SECOND-ORDER CHEMICAL REACTION IN A PACKED COLUMN*

—— EFFECTS OF CONTACT-TIME DISTRIBUTION ——

JOSÉ C. MERCHUK**, KAZUHIRO NAKANISHI, AND FUMITAKE YOSHIDA

Department of Chemical Engineering, Kyoto University, Kyoto

Absorption of carbon dioxide into aqueous solution of sodium hydroxide was studied in a packed column under conditions such that the accompanying reaction was of the second order. In this case the average or volumetric reaction factor for the packed column, i.e. the ratio of the volumetric coefficients for absorption with and without chemical reaction, is complicated by the non-uniform contact-time distribution. However, the assumption of Porter's "long, slow flow paths" model for the contact-time distribution led to a successful correlation for the average reaction factor.

Introduction

Gas absorption with chemical reation has been the subject of a number of investigations, theoretical and experimental.

The factors involved in the performance of equipment for gas absorption with chemical reaction can be grouped into two categories: physicochemical properties, such as diffusivity and reaction rate constants, and hydrodynamic factors such as fluid velocity or gas-liquid contact time. With equipment such as a packed column, in which the local or point value of the mass transfer coefficient such as k_G or k_L is not uniform, the value of the volumetric coefficient of mass transfer such as $k_G a$ or $k_L a$ should be affected by the distribution of the local values of k_G or k_L. In the concept of the effective interfacial area[11,14,15] the situation is simplified by assuming that the effective part of the interface has a uniform k_L or k_G value whereas the remainder of the interface is totally ineffective. Although this concept is practical, it does not represent a real picture of the problem. The distribution of the local values of k_L could be regarded as the distribution of the gas-liquid contact times according to the penetration theory. Thus a more rigorous approach to the problem is to take into account the distribution of contact times as a basis for calculating the average value of $k_L a$. However, it is very difficult to determine directly the contact-time distribution, although some relationships between contact time and liquid residence time have been proposed[5,16]. A more realistic approach would be to assume arbitrarily some form of contact-time distribution and compare experimental results with calculations based on the assumed contact-time distribution.

The present work was undertaken along the latter approach in an attempt to seek an appropriate model for contact-time distribution in the packed column. Experiments were performed on pure physical absorption and on absorption with second-order chemical reaction in a packed column. The latter kind of absorption in the packed column has been studied by very few previous investigators. The total interfacial area was evaluated from data on absorption with pseudo-first-order reaction.

Experimental

A schematic diagram of the experimental apparatus for chemical absorption is shown in **Fig. 1**. The column used, made of transparent acrylic resin, was 10 inches

in diameter and was packed with one-inch carbon Raschig rings to a depth of 33.5cm. Due caution was taken in the design of the gas distributor at the bottom and the liquid distributor at the top so that the end effects due to splashing and spraying were minimized. Both gas and liquid were supplied to the top of the column, i. e. the operation was cocurrent.

In the case of physical absorption tap water and pure carbon dioxide, which was supplied from a cylinder, were fed to the column directly. The flow rate of carbon dioxide was approximately 10 times the rate of absorption. The water rate was 1 to 26m³/m²hr. The water temperature was 29 to 32°C., and the gas temperature was 30 to 33°C.

In the case of absorption with chemical reaction an aqueous solution of sodium hydroxide was supplied to the column from a 1500–litre tank by a centrifugal pump without recirculation, and the air-carbon dioxide mixture was recirculated through the column by a centrifugal blower. Carbon dioxide was supplied from a cylinder to the gas duct continuously through an orifice so as to keep the inlet gas composition constant. Four liquid rates from 3 to 10m³/m²·hr were used. The gas rates were 2800 to 3000kg/m²·hr.

The runs with pseudo-first-order reaction were performed with liquid concentrations around 1 N-NaOH and gas compositions of 8 to 12% CO_2 depending on the liquid rates. In the runs with second-order reaction the NaOH concentration was 0.5 to 1 N, and the gas composition was 12 to 90% CO_2. Due to the heat of reaction liquid and accordingly gas showed temperature rises while they passed through the column. The maximum temperature rise was 4°C. in the liquid and 0.2 °C. in the gas. The gas was cooled by means of a copper coil inserted in the gas recirculating duct.

At the start of a run the liquid rate was kept about 50% higher than the desired value for 5 to 10 minutes and then at the desired value for 15 to 20 minutes. Then, the gas flow was started. The liquid samples were taken after repeated analyses of the inlet gas showed a constant value.

Analysis of the liquid samples in the physical absorption runs was done chemically using aqueous $Ba(OH)_2$ solutions. In the runs with chemical reaction carbonate in the liquid sample was precipitated with $BaCl_2$ solution and free hydroxide was titrated with standard hydrochloric acid. Carbon dioxide in the gas was analyzed by means of an interference gas analyzer for lower concentrations up to 20%. Gas samples containing over 50% CO_2 were withdrawn with a syringe and were analyzed by absorbing CO_2 into a known amount of standard KOH solution contained in an Erlenmeyer flask, to which a toy balloon was attached to prevent escape of the gas, the excess KOH being back-titrated. This method checked well with analysis using the Orsat apparatus.

Calculations

In the calculation based on the data on physical

① Liquid reservoir   ⑥ Gas blower
② Pump   ⑦ Gas flow meter
③ Liquid flow meter   ⑧ CO_2 cylinder
④ Packed column   ⑨ CO_2 flow meter
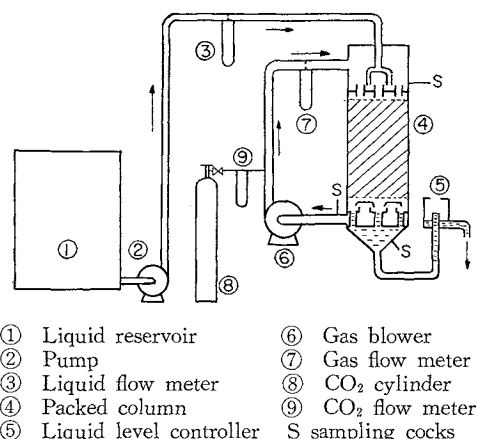⑤ Liquid level controller   S sampling cocks

Fig. 1   Experimental apparatus

absorption, plug flow of liquid in the direction of the column axis was assumed. The $k_L a$ values thus obtained were corrected for temperature to give 25°C. values, using the following relationship proposed by Vivian and King[13].

$$\overline{k_L a} \propto \exp\ (0.019t) \tag{1}$$

when other conditions remain unchanged.

In dealing with the chemical absorption data the gas phase resistance, estimated by use of the correlation of Fellinger[2], was deducted from the overall resistance to obtain the true liquid phase resistance. In estimating the solubility of carbon dioxide in the alkali solutions the method proposed by Van Krevelen and Hoftijzer[12] was adopted. For the diffusivity of carbon dioxide in the alkali solutions the formula proposed by Nijsing et al.[6] was used. The reaction rate constant k for the reaction between dissolved carbon dioxide and OH^- ion was estimated by the equation proposed by Pinsent et al.[7]. In all calculations the alkali concentration used was the arithmetic mean of the concentrations at the top and bottom of the column.

Results and Discussions

Physical absorption data   The $k_L a$ data obtained for the physical absorption runs are plotted against the liquid rate in **Fig. 2**, in which the line for the data of Sherwood and Holloway[16] is also shown. Fair agreement is seen between the two sets of data. Since the chemical absorption runs were carried out in the same column, the present $\overline{k_L a}$ correlation was used as the basis for comparison with the chemical absorption data.

Confirmation of order of reaction   Most of the runs for chemical absorption were carried out under such conditions that the accompanying reaction was of the second order, as aforementioned. If absorption were accompanied by "instantaneous", or extremely rapid, irreversible second-order reaction, the reaction factor i. e. the relative increase in the absorption rate due to chemical reaction, should be given by the following equation proposed by Hatta[3]

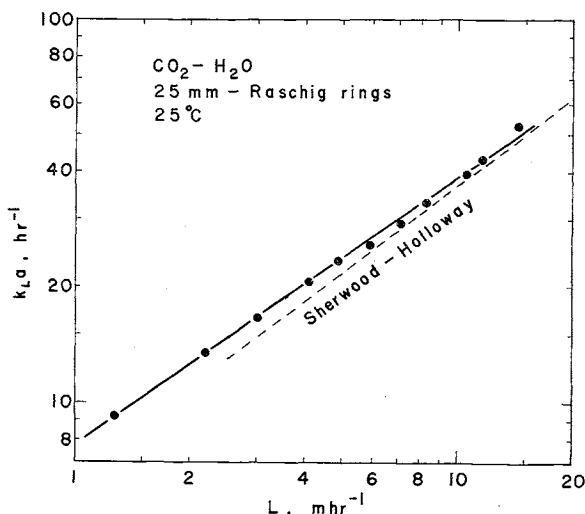$$\beta_\infty = \frac{k_L{}'}{k_L} = 1 + \frac{D_B}{D_A}\frac{C_B}{C_{Ai}} \tag{2}$$
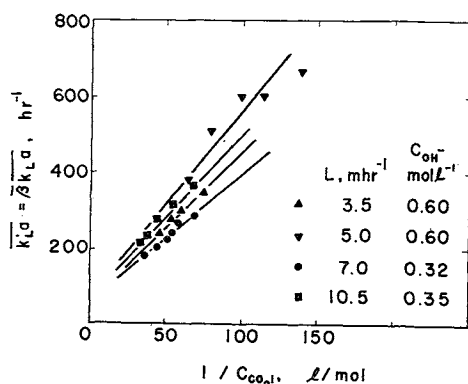
Fig. 2 $k_L a$ for physical absorption

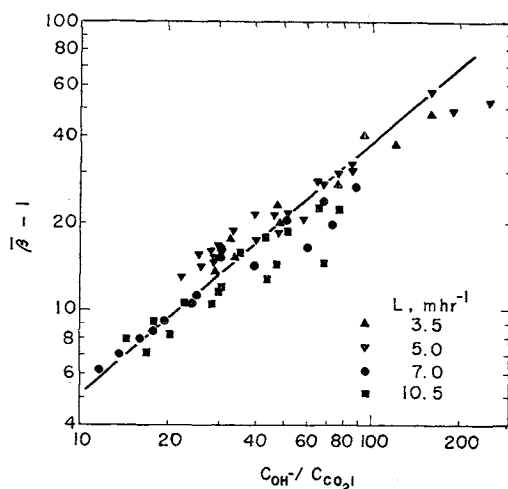Fig. 3   Plot of $\overline{k_L'a}$ vs. $1/C_{CO_2 i}$

Fig. 4   Plot of $(\bar{\beta}-1)$ vs. $C_{OH^-}/C_{CO_2 i}$

On the other hand, if the reaction were pseudo-first-order, β should be practically equal to γ, for the range where γ is greater than 5 [15], i. e.

$$\beta = \frac{k_L'}{k_L} = \gamma = \frac{(kC_BD_A)^{0.5}}{k_L} = \left(\frac{\pi}{4}kC_B\theta\right)^{0.5} \quad (3)$$

In this case, β or k_L' should be independent of C_{Ai},

the concentration of dissolved gas at the interface. **Fig. 3**, in which $k_L'a$ values for the runs with fixed values of liquid rates and C_{OH^-} are plotted against the reciprocals of C_{Ai}, indicates that in these runs the accompanyin greaction was not of pseudo-first-order. At equal concentrations of OH^-, $k_L'a$ values are higher for the runs at higher liquid rates, since k_La increases with the liquid rate.

Fig. 4 is a log-log plot of $(\bar{\beta}-1)$ against $C_{OH^-}/C_{CO_2 i}$ for all the chemical absorption runs. Such plots were used by Yoshida and Miura[15] and other previous investigators. If the accompanying reaction were extremely rapid, such a plot should result in a straight line with a slope of unity according to Eq. (2). Although there exists no actual case where the slope is unity, the faster the accompanying reaction, the closer the slope to unity. The slope of the line in **Fig. 4** is 0.88, indicating that the accompanying reaction was fairly but not extremely rapid. In the figure several datum points considerably below the line are for runs with high OH^- concentrations. This seems to imply that those runs represent the intermediate case between pseudo-first-order and second-order reactions.

Correlation based on Porter's model   The theoretical relationship between β and γ is usually represented by a family of curves with a parameter β_∞, i. e. the upper limit of β set by diffusion of some species in the liquid to the reaction site. Porter[8] proposed the following empirical approximation for the relationship between β and γ, which covers both the pseudo-first-order and second-order regimes.

$$\beta_r = 1 - \exp(-\gamma_r) \quad (4)$$

where

$$\beta_r = \frac{(\beta - 1)}{(\beta_\infty - 1)} \quad (5)$$

and

$$\gamma_r = \frac{(\gamma - 1)}{(\beta_\infty - 1)} \quad (6)$$

Porter has shown that Eq. (4) compares well with the numerical solution of Brian et al.[1] for the entire second-order regime. Application of Eq. (4) to the prediction of the rate of gas absorption with second-order reaction in packed columns is complicated by the local variation of k_L due to the distribution of gas-liquid contact times θ. To avoid this complication Porter has derived the following ralationship for the volumetric reaction factor, $\bar{\beta}$, i. e. β averaged over the entire interface.

$$\bar{\beta} = \frac{\overline{k_L'a}}{k_La} = \frac{\overline{k_L'}}{k_L}$$
$$= 1 + (\beta_\infty - 1)\left\{1 - F(\alpha)\exp\left[-\frac{1}{(\beta_\infty - 1)}\right]\right\} \quad (7)$$

where

$$F(\alpha) = \frac{\left\{\int_{\theta_s}^{\theta_1} f(\theta)\theta^{-0.5}\exp\left(-\alpha\theta^{0.5}\left[\int_{\theta_s}^{\theta_1} f(\theta)\theta^{-0.5}d\theta\right]\middle/\left[\int_{\theta_s}^{\theta_1} f(\theta)d\theta\right]\right)d\theta\right\}}{\int_{\theta_s}^{\theta_1} f(\theta)\theta^{-0.5}d\theta} \quad (8)$$

in which

$$\alpha = \frac{\bar{r}}{(\beta_\infty - 1)} \qquad (9)$$

and $f(\theta)$ is defined by

$$a = \int_{\theta_s}^{\theta_1} f(\theta) d\theta \qquad (10)$$

$F(\alpha)$ depends only on α and the contact-time distribution function $f(\theta)$. For a given contact-time distribution under fixed hydrodynamic conditions, $F(\alpha)$ can be correlated by an experimental plot against α, which involves physico-chemical constants, k, C_B, and D_A. Thus, for given equipment and given hydrodynamic conditions, once an experimental plot of $F(\alpha)$ vs. α has been established for one system, the rate of absorption with second-order reaction may be predicted for any other system by calculating the value of α for that system.

In the absence of experimental information on the contact-time distribution, Porter[8] assumed four hypothetical models of contact-time distribution, obtained four expressions for $da/d\theta$ as function θ, and thence the relationships between $F(\alpha)$ and α for the four cases. Unfortunately, no experimental data for packed columns were available to him to test the validity of his models. What he did was only to test Eq. (4) using the literature data for uniform contact-time equipment such as the wetted-wall column.

The present data on absorption with second-order reaction were compared with the calculations based on the four models proposed by Porter. To do this, the total gas-liquid interfacial area a must be known, since $\bar{k}_L$ obtained by dividing $k_L a$ by a is required to evaluate $\bar{r}$ and α. **Fig. 5** shows the total interfacial area, determined by the method of Yoshida and Miura[15] using the pseudo-first-order reaction between dissolved CO_2 and $NaOH$, as a function of the liquid rate.

Fig. 6, in which $F(\alpha)$ values calculated from the present data are plotted against α, also shows the curves representing the four models as indicated. It is seen that the "long, slow flow paths" model fits the present data best. Curves representing other models proposed by Porter are also shown in the figure for comparison. The "long, slow flow paths" model assumes that the liquid over a piece of packing flows most rapidly down the shortest flow path and less rapidly at the edges of the actively wetted surface, where the flow path is

longer; and that the liquid surface velocity is inversely proportional to the length of flow path between the mixing points at junctions of packing pieces. From this assumption Porter has derived the following relationship for the contact-time distribution.

$$\frac{da}{d\theta} = \frac{1}{4\bar{\theta}} \quad \text{for} \quad 0 > \theta > 4\bar{\theta} \qquad (11)$$

where $\bar{\theta}$ is the mean Higbie contact time which is defined by

$$\bar{k}_L = \frac{\bar{k}_L a}{a} = 2\left(\frac{D_A}{\pi}\right)^{0.5} \frac{1}{\bar{\theta}^{0.5}} \qquad (12)$$

With the assumption of the "long, slow flow paths" model, he obtained from Eq. (8).

$$F(\alpha) = [1 - \exp(-2\alpha)]/(2\alpha) \qquad (13)$$

For the $F(\alpha)$ vs. α relationships based on other models reference should be made to the original paper by Porter[8].

In **Fig. 7** the average values of $\bar{\beta}_r$ i. e. $(\bar{\beta}-1)/(\beta_\infty -1)$, calculated from the present data, are plotted against $\bar{r}_r$ i. e. $(\bar{r}-1)/(\beta_\infty-1)$. All of the datum points fall below the solid curve representing Eq. (4). This could be explained in a simple intuitive way. Suppose that the gas-liquid interface consists of two regions, one with a high surface liquid velocity, short contact-time, k_L value, and accordingly low r value, and the other with a lower surface liquid velocity, long contact-time, low k_L value and accordingly high r value. The two regions should both lie on the curve, considerably apart from each other, their locations depending on r values. The point representing an average value of $\bar{\beta}$ should lie on the chord joining the two points, the location of the point depending on the relative magnitudes of the areas of the two regions. It is evident that even if the variation of local k_L values is
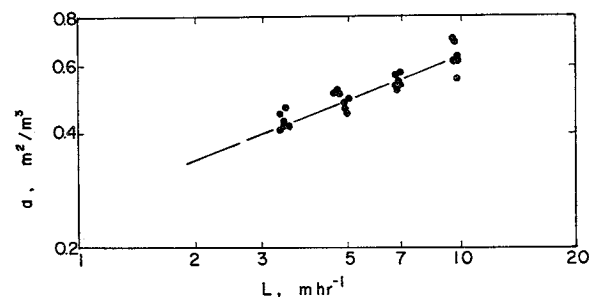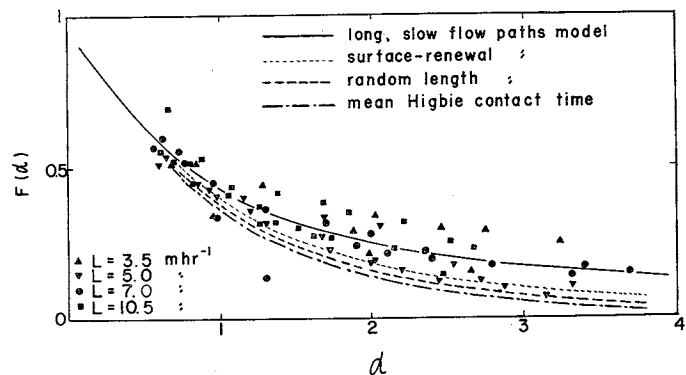

Fig. 5   Total interfacial area vs. liquid rate

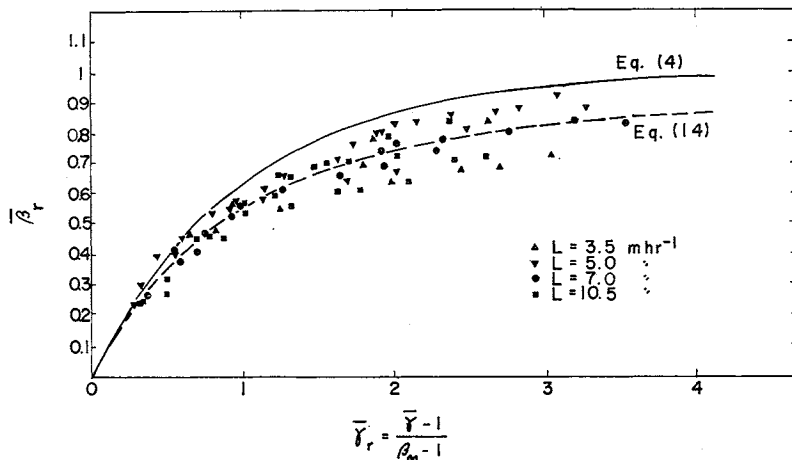Fig. 6   Experimental values of $F(\alpha)$ compared with calculations

Fig. 7   Plot of β_r vs. γ_r

continuous, the point for the average $\bar{\beta}$ value will be somewhere on the chord, i. e. below the curve representing Eq. (4). For details of this discussion see reference[9]. The liquid rate does not seem to affect the contact time distribution, since no trend with the liquid rate is seen in Fig. 6.

From Eqs. (4), (6), (7), (9), and (13) one can obtain the following equation:

$$\bar{\beta}_r = 1 - \left[\frac{1 - \exp(-2\alpha)}{2\alpha}\right]\exp\left(\frac{1}{\beta_\infty - 1}\right) \quad (14)$$

where

$$\alpha = \gamma_r + \frac{1}{\beta_\infty - 1} \quad (14a)$$

The broken line Fig. 7, which represents Eq. (14), fits the experimental datum points fairly well, as is expected.

Conclusions

Experimental data on the rate of gas absorption with second-order reaction in a packed column have shown that the volumetric reaction factor $\bar{\beta}$, defined as $\overline{k_L'a}/\overline{k_La}$, can be predicted by Eq. (14), which was derived from Eq. (7) proposed by Porter and one of his assumptions about the contact-time distribution, i. e. the "long, slow flow paths" model.

Acknowledgement

Nomenclature

a = total gas-liquid interfacial area per unit of packed volume [m²/m³]
C = molar concentration in the liquid [kg-mole/m³]
D = diffusivity in liquid phase [m²/hr]
$F(\alpha)$ = correlating function defined by Eq. (8)
$f(\theta)$ = contact-time distribution function described by Eq. (10)
k = second-order reaction velocity constant [m³/kg-mole·hr]
k_G = gas phase coefficient of mass transfer, local value [kg-mole/m²·hr·atm]
$\overline{k_La}$ = volumetric coefficient of mass transfer without chemical reaction [hr⁻¹]
k_L = liquid phase coefficient of mass transfer without chemical reaction, local value [m/hr]
k_L' = liquid phase coefficient of mass transfer with chemical reaction, local value [m/hr]
$\overline{k_L'a}$ = volumetric coefficient of liquid phase mass transfer with chemical reaction [hr⁻¹]
t = temperature [°C]
α = $\bar{\gamma}/(\beta_\infty - 1)$
β = reaction factor, i. e. relative increase in absorption rate due to chemical reaction
β_∞ = upper limit of β set by diffusion of some species in liquid
γ = $(kC_BD_A)^{0.5}/k_L$
γ_r = $(\gamma - 1)/(\beta_\infty - 1)$
θ = contact time [hr]
$\bar{\theta}$ = mean Higbie contact time defined by Eq. (12) [hr]
θ_1, θ_s = limits of hypothetical contact-time distribution of Eq. (10)

Subscripts
A = absorbed gas, i. e. CO_2
B = reactant, i. e. NaOH or OH⁻
i = interface

Superscripts
— = average value over the total interfacial area based on distribution of contact times

Literature Cited

1) Brian, P. L. T., J. F. Hurley, and E. H. Hasseltine,: *A. I. Ch. E. J.*, **7**, 226 (1961)
2) Fellinger, L: Sc. D. Thesis, Mass. Inst. Technol. (1941)
3) Hatta, S.: Technol. Repts. Tohoku Imp. Univ., **8**, 1 (1928-9)
4) Higbie, R.: *Trans. Am. Inst. Chem. Engrs.*, **31**, 365 (1935)
5) Koppel, L. B., R. D. Patel and J. T. Holmes: *A. I. Ch. E. J.*, **12**, 941 (1966)
6) Nijsing, R. A. T. O., R. H. Hendriks and H. Kramers: *Chem. Eng. Sci.*, **10**, 88 (1959)
7) Pinsent, B. R. W., L. Pearson and F. J. W. Roughton: *Trans. Faraday Soc.*, **52**, 1512 (1956)
8) Porter, K. E.: *Trans. Instn Chem. Engrs.*, **44**, T 25 (1966)
9) Ronco, J. J. and J. C. Merchuk: Genie Chimique, **96**, 71 (1966)
10) Sherwood, T. K. and F. A. L. Holloway: *Trans. Am. Inst. Chem. Engrs.*, **36**, 39 (1940)
11) Shulman, H. L., et al.: *A. I. Ch. E. J.*, **1**, 247, 253, 259 (1955)
12) Van Krevelen, D. W. and P. J. Hoftijzer: XXI Congr. Int. Chim. Industr., 168 (1948)
13) Vivian, J. E. and C. J. King: *A. I. Ch. E. J.*, **10**, 221 (1964)

14) Yoshida, F. and T. Koyanagi: *A. I. Ch. E. J.*, 8, 309 (1962)

15) Yoshida, F. and Y. Miura: *A. I. Ch. E. J.*, 9, 331 (1963)

16) Zwietering, N. T: *Chem. Eng. Sci.*, 11, 1 (1959)

EFFECTIVENESS FACTOR AND TEMPERATURE PROFILE OF A SINGLE SPHERICAL CATALYST PELLET WITH SURFACE TEMPERATURE DISTRIBUTION*

——HYDROGENATION OF ETHYLENE——

SHIGEO GOTO AND NORIYOSHI MORITA

Dept. of Chemical Engineering, Nagoya University, Nagoya

Hydrogenation of ethylene on a single spherical catalyst in a tubular reactor was carried out at ambient temperature of 35~75°C and with volumetric velocity of reactive gases of 10~40 cm³ (18 °C, 1 atm)/sec. The conversion at the outlet and the temperatures at the center and at various azimuthal angular positions to the stream on the outer surface of the catalyst were measured.

The method of Bischoff to evaluate effectiveness factor for catalyst particle with non-uniform surface temperature was extended to include transport effects of fluid film, applying the method presented previously by the present authors. Numerical values of the effectiveness factor obtained by various methods are compared and discussed.

Introduction

Many analytical studies have been made of the effectiveness factor of isothermal and nonisothermal catalysts, but few were done experimentally[5]. Experimental work involves many difficulties, e. g., accurate estimation of the effective diffusivity and the thermal conductivity are required ; the remarkable influences of the external heat and mass transfer must be taken into consideration. Moreover, the environment around the catalyst particle may not be uniform and there may be temperature and concentration distributions on the external surface of the catalyst.

In a previous paper[3], we presented a method to calculate effectiveness factor in view of external and internal transport effects and compared results with published experimental data. Recently, Bischoff[1] showed how the temperature profile and the effectiveness factor of a spherical catalyst pellet could be obtained when a temperature distribution existed on the external surface of the catalyst.

In this paper, a single spherical catalyst pellet was used for the hydrogenation of ethylene, and temperature distribution and effectiveness factor were measured. The method of Bischoff was applied to our method to evaluate effectiveness factor, and compared with experimental results.

Experimental

The experimental apparatus is the same as used previously[4], except for the reactor. Details of the reactor are shown in **Figs. 1a, b,** and **c.** The catalyst pellet is supported by pivots made of thin glass rod as shown in Fig. 1a. The pivots allow the catalyst to rotate easily around the horizontal axis by handling the thermocouple wires and also serve to minimize thermal conduction through the glass rod. The rod is fixed to the cap of the reactor by epoxy resin. The thermocouple wires are arranged to the cap as shown in Fig. 1b. The inner glass tube holds the wires fixed by epoxy resin and can move up and down in the outer glass and polyethylene tube. The movment is made smooth and gas tight by silicone grease.

The catalyst has a hole smaller than 1mm dia. through the center, as shown in Fig. 1c. Two Alumel vs. Chromel thermocouples of 0.1mm dia. are inserted in the hole, one being fixed at the junction at the center and the other at the external surface. The hole is then filled with fire-clay binder. The catalyst is supported by the pivots perpendicularly to the hole, so the catalyst can rotate around the axis by handling the thermocouple wires. Thus, the temperature can be measured at any azimuthal angular position to the fluid stream between 10° and 170°.

The spherical catalyst was prepared as follows: Harshaw nickel catalyst, Ni-0101T (1/8″ cylindrical, 44% Ni present as hydrate mounted on Kieselguhr) was pulverized and mixed with Kieselguhr as diluent and a binder (magnesium stearate : sodium carbox-